Online ISSN 1848-3380, Print ISSN 0005-1144
ATKAFF 54(1), 9–18(2013)

Wataru Maebashi, Kazuaki Ito, Makoto Iwasaki

Practical Feedback Controller Design for Micro-Displacement Positioning in Table Drive Systems

DOI 10.7305/automatika.54-1.310
UDK 681.532.8.013.037-23; 531.4.083.98
IFAC 3.2; 2.6

Original scientific paper

This paper presents a practical feedback controller design of a ball screw-driven table system for the micro-displacement positioning. Friction of the mechanism in the micro-displacement region has nonlinear elastic properties, unlike Coulomb and/or viscous friction in the macro-displacement, resulting in different positioning responses and frequency characteristics of the plant depending on the regions. In this paper, at first, a numerical simulator with a rolling friction model is adopted to reproduce the positioning behaviors in the micro-displacement region. Based on the simulator, the stability condition of positioning in the region is clarified on the basis of frequency characteristics and, then, appropriate parameters of feedback controller are practically designed to satisfy the required positioning performance. Effectiveness of the proposed design has been verified by a series of experiments using a prototype of ball screw-driven table positioning device.

Key words: Precision positioning, Micro-displacement region, Nonlinear friction, Stability condition

Praktična sinteza regulatora za precizno pozicioniranje sustava pomične podloge. U radu je prikazana sinteza regulatora s povratnom vezom u sustavu za precizno linearno pozicioniranje pomične podloge pomoću kugličnih ležajeva. Za razliku od uobičajenih modela Coulombova i/ili viskoznog trenja, trenje razmatranog sustava ima izrazito nelinearna svojstva u području mikro-pomaka, što za posljedicu ima različite odzive pozicioniranja i frekvencijski karakteristike, ovisno o radnom području. U radu je prvo razvijeno numeričko simulacijsko okruženje zasnovano na modelu trenja kotrljanja u svrhu simuliranja ponašanja sustava pozicioniranja u području mikro-pomaka. Potom je, zasnivajući se na simulacijskom okruženju, pomoću frekvencijske karakteristike razjašnjen problem stabilnosti sustava u promatranom radnom području te su odabrani odgovarajući parametri regulatora koji poštuju uvjet stabilnosti i zadovoljavaju željenu kvalitetu odziva. Sinteza regulatora provedena je vodeći računa o praktičnoj primjenjivosti postupka. Učinkovitost predložene sinteze potvrđena je nizom eksperimenata na prototipu sustava za precizno linearno pozicioniranje pomične podloge pomoću kugličnih ležajeva.

Ključne riječi: Precizno pozicioniranje, područje mikro-pomaka, nelinearno trenje, uvjet stabilnosti

1 INTRODUCTION

High precision motion performance in the micro-displacement region (up to about 100 μm; "micro region" in the following) is indispensable to provide the fine positioning with short stroke references and/or the desired settling performance for varieties of industrial and/or consumer mechatronic systems, such as data storage devices, machine tools, electronics manufacturing machines, and industrial robots. In order to achieve the required performance, disturbance suppression capabilities are generally important properties for the controllers, since nonlinear components in the mechanisms, such as friction and elasticity, behave as more complicated disturbances than the ones in the macro-displacement region ("macro region" in the following), which lead to deterioration and dispersion in the positioning accuracy [1–3]. In the references [1, 2], the friction behaviors were clearly categorized in the micro and macro regions, where nonlinear friction properties with elasticity led to different characteristics of plant mechanism among the regions due to the different behaviors as disturbance in the plant. Expansion of the servo bandwidth in feedback control systems, therefore, should be one of essential approaches to achieve the higher positioning performance by improving the disturbance suppression. Although the higher gain feedback control allows the servo bandwidth to be wider, upper values of the gains are generally limited by the system stability due to mechanical vibrations, dead time (phase delay) properties, etc. Feedforward control frameworks, on the other hand, are also promising, where precise disturbance mod-

els and/or disturbance estimators can compensate for the nonlinearities. In the feedforward control manners, however, it is essentially difficult to achieve robust properties against variations in the disturbances.

Friction in the drive mechanism especially has a nonlinear elastic property in the micro region [4–7], unlike Coulomb and/or viscous friction in the macro region [8], resulting in different positioning responses as well as variations in frequency characteristics depending on the regions. In the reference [4], typical friction models (static, Dhal, LuGre, Leuven models) were analytically compared to verify the friction model-based compensation in accurate low-velocity tracking. Rolling friction characteristics were clearly modeled and parameterized by optimization techniques such as genetic algorithms in the reference [5], being able to compensate for friction in linear motor-driven table stage systems. In addition, friction models (generalized Maxell-slip and variable length spring models) were applied in the references [6, 7], to improve circular trajectory performances in machine tool drives. On the other hand, in the positioning with short stroke references and/or at the settling regions, it is well-known that the nonlinear elastic friction force leads to "slow responses" with poor settling performance [7, 9]. In the reference [9], analytical examinations on the slow response, i.e., how the elastic friction behaves and affects to frequency properties of plant system, were especially clarified, as well as the friction model-based compensation approach.

Under the above background, a practical feedback controller design for the micro-displacement positioning in table drive systems is presented in this paper, where the motion performance can be improved by focusing on plant dynamics with friction behaviors as well as stability analyses of the feedback system in the target region. Notice here that this approach stands on different points of friction compensation view from the conventional ones, i.e., the improvement of disturbance suppression performance can be realized only by parameter design in the simple feedback control framework. At first, a numerical simulator with a rolling friction model is adopted to reproduce the positioning behaviors in the micro region. Based on the simulator, the stability condition of positioning in the region is clarified on the basis of frequency characteristics and, then, appropriate parameters of feedback controller are practically designed to satisfy the required positioning performance.

Effectiveness of the proposed design is verified by a series of positioning experiments using a prototype of ball screw-driven table positioning device, presenting a practical controller design for the high precision motion in varieties of mechatronic systems including the micro-displacement positioning.

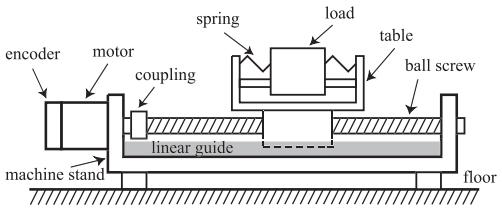

Fig. 1. Ball screw-driven table positioning system

The contents of paper are organized as follows: In Section 1, background and outline of the research are clearly stated as the introduction. Following to the introduction, a target position control system for a ball screw-driven table in the research is explained in Section 2, where mechanisms of a prototype and control specifications, position control system, and basic positioning performances are presented. In Section 3, positioning performances are numerically analyzed in both frequency and time domains, by introducing a rolling friction model in the micro region, where the analyses suggest how the feedback controller should be designed. According to the analytical examinations, the feedback controller is re-designed and, then, the positioning performances are numerically and experimentally evaluated in Sections 4 and 5. Finally, the paper is concluded in Section 6.

2 POSITION CONTROL SYSTEM

2.1 Ball Screw-driven Table System

Figure 1 shows a structural configuration of the target ball screw-driven table positioning system as a prototype. A table with a flexible load is driven by a motor (rated torque of 1.27 Nm) through a ball screw, where the drive mechanism is mounted on a machine stand. The table is guided by rolling ball guides (linear guides) on the machine stand, where the rolling friction [7,9,10] is generated at contact points between rolling elements and the guides with lubricant grease, deteriorating the positioning performance. The machine stand vibration (the primary mode at 33 Hz), on the other hand, is excited due to the reaction force of motor torque during acceleration and deceleration motions, while the flexible load also excites a resonant vibration (the 2^{nd} mode at 65 Hz), that simulates vibratory mechanisms in a variety of industrial positioning devices.

Solid lines in Fig. 2 show a bode characteristic of the plant system (from motor torque reference to motor position). In the characteristic, the primary and 2^{nd} vibration modes that directly lead to vibratory responses in positioning are clearly observed, while higher vibration modes above 200 Hz exist that affect the robust stability in FB system. In the following controller design, a linear nominal plant model P_r can be formulated as follows, including

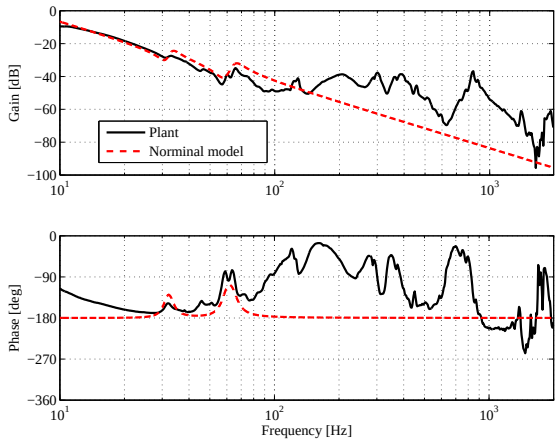

Fig. 2. Bode characteristics of plant and nominal model

Table 1. Parameters of nominal plant model

J_m	5.3×10^{-4} [kgm^2]		
k_{t1}	200 [1/kgm^2]	k_{t2}	500 [1/kgm^2]
ω_{t1}	$2\pi \times 33.0$ [rad/s]	ω_{t2}	$2\pi \times 65.0$ [rad/s]
ζ_{t1}	0.06	ζ_{t2}	0.075

the primary and 2$^{\rm nd}$ vibration modes:

$$P_r(s) = \frac{1}{J_m s^2} + \sum_{i=1}^{2} \frac{k_{ti}}{s^2 + 2\zeta_{ti}\omega_{ti}s + \omega_{ti}^2}, \qquad (1)$$

where J_m: motor moment of inertia, ω_{ti}: natural angular frequency of i-th vibration mode, ζ_{ti}: damping coefficient, and k_{ti}: vibration mode gain, respectively. Broken lines in Fig. 2 correspond to the bode characteristic of P_r in eq.(1), while table 1 lists the parameters of P_r.

The table position is indirectly detected by a motor encoder (equivalent resolution of 0.5 μm/pulse on table side), and is controlled in a semi-closed position control manner by a DSP (Digital Signal Processor, control sampling period of T_s) and a servo amplifier.

In the following, an S-shaped motor position reference with amplitude of 40 motor encoder pulses (equivalent to 20 μm) is given as a typical short stroke positioning motion, where the position should be settled with the accuracy of $\pm$10 pulses with settling time of 176 sampling periods (176 $T_s \simeq 45$ ms) as the typical specification. Notice here that the position and time are represented by encoder pulses and control sampling numbers as normalized values.

2.2 2-Degrees-Of-Freedom Positioning System

In this system, a robust 2-degrees-of-freedom (2DOF) control system based on the coprime factorization description [11] is applied to achieve the desired positioning performance. Feedback controller consists of a well-known P-PI (proportional for position, and proportional plus integral for velocity) controller and a robust filter, where the robust filter ensures the robustness against the high frequency vibration modes. Feedforward compensation based on the mathematical plant model, on the other hand, provides the fast and precise positioning property.

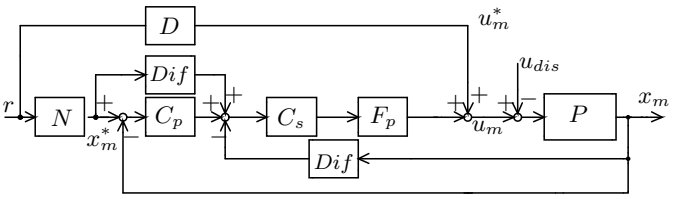

Fig. 3. Block diagram of 2-degrees-of-freedom positioning system

Table 2. Parameters of N, D, and $1/F$

n_0	7.17×10^9	d_0	0.00
n_1	6.78×10^6	d_1	0.00
n_2	2.40×10^5	d_2	3.80×10^6
n_3	9.92×10^1	d_3	3.60×10^3
n_4	1.37	d_4	1.12×10^2
		d_5	4.57×10^{-2}
		d_6	5.30×10^{-4}
ω_{F1}	$2\pi \times 55$ [rad/s]	ζ_{F1}	1.0
ω_{F2}	$2\pi \times 60$ [rad/s]	ζ_{F2}	1.0
ω_{F3}	$2\pi \times 60$ [rad/s]	ζ_{F3}	1.0

Figure 3 shows a block diagram of the 2DOF positioning system for the target table drive system, where P: actual plant dynamics of motor position for torque reference, N and D: feedforward compensators, C_p and C_s: position and velocity feedback compensators, F_p: robust filter, r: motor position reference, x_m^*: ideal motor trajectory, x_m: actual motor position, u_{dis}: disturbance, u_m^*: feedforward torque, u_m: torque reference, Dif: operation of differentiation, respectively. Notice here that this positioning controller requires a precise tracking performance for x_m^* given as the output of N, although the original control purpose is specified as a point-to-point positioning.

The feedforward compensators N and D are designed by the coprime factorization expression framework, where the nominal plant model P_r with the primary and 2$^{\rm nd}$ vibration modes is factorized as:

$$P_r(s) = \frac{N_r(s)}{D_r(s)} \qquad (2)$$
$$= \frac{n_4 s^4 + n_3 s^3 + n_2 s^2 + n_1 s + n_0}{d_6 s^6 + d_5 s^5 + d_4 s^4 + d_3 s^3 + d_2 s^2 + d_1 s + d_0},$$

Table 3. Parameters of F_p

ω_1	$2\pi\times1200$ [rad/s]	ζ_1	0.700
ω_{n2}	$2\pi\times200$ [rad/s]	ζ_{n2}	0.030
ω_{d2}	$2\pi\times202$ [rad/s]	ζ_{d2}	0.100
ω_{n3}	$2\pi\times280$ [rad/s]	ζ_{n3}	0.040
ω_{d3}	$2\pi\times280$ [rad/s]	ζ_{d3}	1.000
ω_{n4}	$2\pi\times440$ [rad/s]	ζ_{n4}	0.060
ω_{d4}	$2\pi\times440$ [rad/s]	ζ_{d4}	1.000
ω_{n5}	$2\pi\times860$ [rad/s]	ζ_{n5}	0.003
ω_{d5}	$2\pi\times860$ [rad/s]	ζ_{d5}	1.000

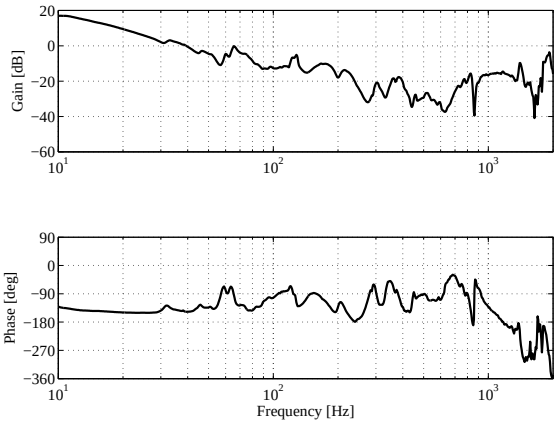

Fig. 4. Bode characteristic of open loop system

$$N(s) = \frac{N_r(s)}{F(s)},\ D(s) = \frac{D_r(s)}{F(s)}, \tag{3}$$
$$\frac{1}{F(s)} = \prod_{i=1}^{3} \frac{{\omega_{Fi}}^2}{s^2 + 2\zeta_{Fi}\omega_{F_i}s + {\omega_{Fi}}^2},$$

where $1/F$ is a 6th-order low pass filter with its bandwidth of 60 Hz, which allows N and D to be proper. Table 2 lists the parameters of N_r, D_r, and $1/F$.

C_p and C_s consist of the following P-PI compensation:

$$C_p(s) = K_{pp}, \tag{4}$$
$$C_s(s) = K_{sp} + \frac{K_{si}}{s}. \tag{5}$$

Compensator gains are set as of K_{pp} = 73.0 [rad/s], K_{sp} = 0.15 [kgm^2/s], and K_{si} = 10.1 [kgm^2/s^2] (defined as "conventional case" in the later examinations). From the plant bode characteristic in Fig. 2, since the primary and 2$^{\rm nd}$ vibration modes can be compensated by the feedforward compensation, higher vibration modes above 200 Hz should be suppressed by the robust filter. The following robust filter F_p, therefore, is designed by serially-connected four notch filters (with notch frequencies of 200, 280, 440, and 860 Hz) and a low path filter (1200 Hz), that ensures the system stability for the higher vibration modes than the 3$^{\rm rd}$ mode in Fig. 2.

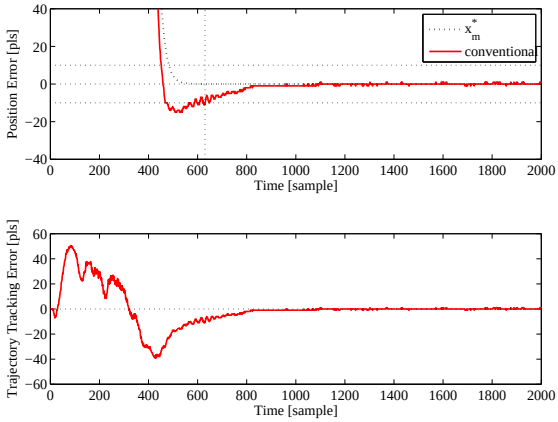

Fig. 5. Response waveforms of conventional system for S-shaped position reference in macro region (reference amplitude of 40000 pulses)

$$F_p(s) = \frac{\omega_1^2}{s^2 + 2\zeta_1\omega_1 s + \omega_1^2} \times \prod_{i=2}^{5} \frac{{\omega_{di}}^2}{{\omega_{ni}}^2} \cdot \frac{s^2 + 2\zeta_{ni}\omega_{ni}s + \omega_{ni}^2}{s^2 + 2\zeta_{di}\omega_{di}s + \omega_{di}^2}. \tag{6}$$

Table 3 lists the parameters of F_p, while an open characteristic of the feedback system with the robust filter F_p is depicted in Fig. 4.

Nonlinear friction as the disturbance u_{dis}, on the other hand, should be compensated to improve the tracking performance, especially in the micro-displacement motion.

2.3 Positioning Performance of Conventional System

In order to evaluate the control performance of the conventional system in the macro and micro regions, S-shaped position references r whose amplitude of 40000 pulses for the macro and 40 pulses for the micro are comparatively applied to the system. Figures 5 and 6 show comparative response waveforms in the macro and micro regions, where the top of each figure shows the response waveform of position error ($r - x_m$), and the bottom shows the trajectory tracking error ($x_m^* - x_m$). In the figures, solid lines indicate the actual positioning responses and the dotted line in the tops indicates x_m^*, while vertical dotted lines in the tops denote the target settling time (630 samples for macro and 176 samples for micro), and horizontal dotted lines in the tops denote the target settling accuracy of ±10 pulses. Although the conventional control achieves the required response in the macro case, the slow response is clearly

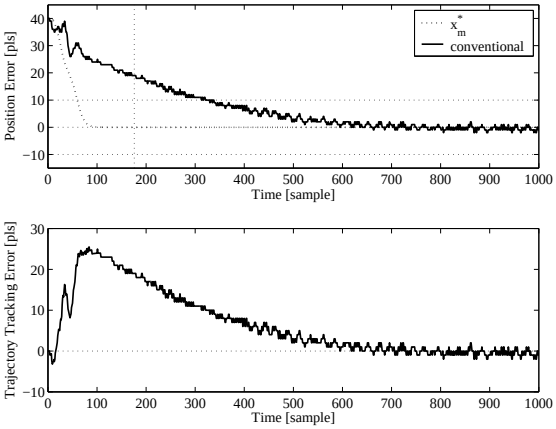

Fig. 6. Response waveforms of conventional system for S-shaped position reference in micro region (reference amplitude of 40 pulses)

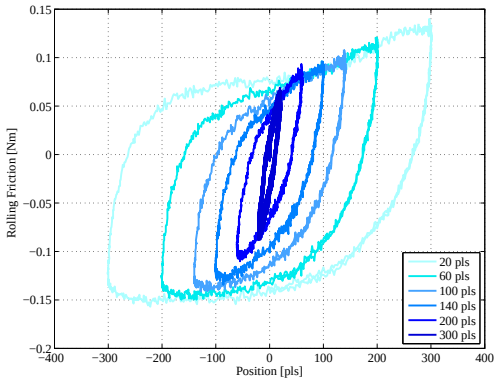

Fig. 7. Rolling friction characteristics

appeared in the micro case due to the effect of nonlinear friction in the region. In addition, notice here that the responses at around the settling region in each case behave in different ways, i.e. with overshoot response in the macro region while without overshoot response in the micro region.

3 NUMERICAL SIMULATION OF POSITIONING PERFORMANCE IN MICRO REGION

3.1 Rolling Friction Modeling

As mentioned above, the nonlinear friction deteriorates the tracking performance for the target trajectory in positioning, resulting in poor settling characteristics. Figure 7 shows an example of friction values for motor position in the target table drive system, where the friction was detected by a disturbance observer during sinusoidal motor position profiles (with low frequency of 0.05 Hz) for different amplitude cases (10 to 300 pulses). In the figure, the friction definitely has nonlinear elastic properties with hysteresis in the displacement regions. These nonlinear elastic characteristics affect the positioning performance as the nonlinear disturbance, especially at the starting and/or settling motion as well as in the micro-displacement positioning. Effects of the friction on the positioning performance, therefore, should be precisely analyzed and compensated to improve the control performance.

One of mathematical models to reproduce the friction behavior is a "rolling friction model" formulated as follows [9, 10]:

$$g(\xi) = \begin{cases} \dfrac{1}{2-n}\{\xi^{n-1} - (n-1)\xi\} : n \neq 2 \\ \xi(1 - \ln \xi) : n = 2 \end{cases}, \quad (7)$$

$$F_r(\delta) = \begin{cases} \mathrm{sgn}(v_m)(2T_{fc}g(\xi) - F_{r0}) \\ \quad : |\delta| < x_r \text{ and } |F_r| < T_{fc} \\ \mathrm{sgn}(v_m)T_{fc} \\ \quad : |\delta| \geq x_r \text{ or } |F_r| \geq T_{fc} \end{cases}, \quad (8)$$

$$\delta = |x_m - \delta_0|, \quad \xi = \frac{\delta}{x_r}, \quad (9)$$

where F_r: rolling friction, T_{fc}: Coulomb friction, δ: motor displacement after reverse motion, ξ: intermediate variable, x_r: displacement of rolling region, n: variable for hysteresis, F_{r0}: rolling friction at reverse motion, δ_0: motor displacement at reverse motion, $\mathrm{sgn}(\cdot)$: sign function, and v_m: motor velocity, respectively. The model parameters are experimentally determined as T_{fc} = 0.1125 Nm, x_r = 300 pulses, and n = 1.6 by try and error processes. Figure 8 evaluates the rolling friction model output in a case of motor sinusoidal amplitude of 100 pulses with an internal hysteresis loop at around the origin. From the figure, the identified model can reproduce the actual rolling friction behaviors.

3.2 Numerical Simulation of Positioning

Figure 9 shows comparative response waveforms of position error (top) and trajectory tracking error (bottom), where red lines indicate the numerical simulation responses using the identified rolling friction model described above, and black lines indicate the experimental results. From the figure, the actual responses can be accurately reproduced by the simulation and, as a result, this comparison clearly states that the slow response in the micro region is caused by the rolling friction properties.

3.3 Frequency Characteristics in Micro Region

Effects of the friction in the frequency domain should be also clarified to examine the positioning performance in

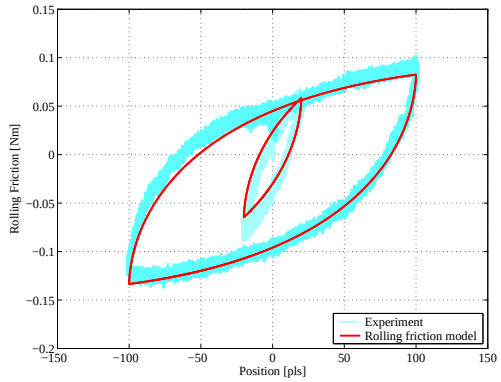

Fig. 8. Rolling friction model output

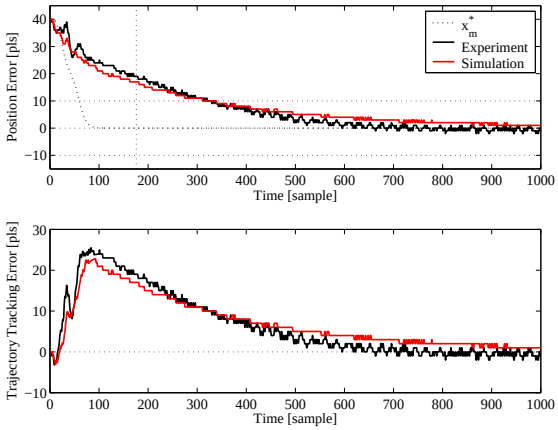

Fig. 9. Numerical simulation waveforms for S-shaped position response in micro region (reference amplitude of 40 pulses)

the micro region. Swept sinusoidal motor position references with amplitude from 20 to 300 pulses were applied to the position control system, to obtain frequency characteristics of the plant in the micro region. Figure 10 shows bode plots of motor position for motor torque reference in the micro region, where broken lines (macro) are measured with large position amplitude (i.e., bode characteristics in the macro region). From the plot, the position amplitude drastically affects the plant dynamics especially in low frequency range up to 30 Hz, in both gain and phase characteristics. In the low frequency range, the friction has a nonlinear elastic component, thus resulting the gain variations and phase lead characteristics for difference in position amplitude. This examination gives that the control bandwidth can be expanded more in the micro region due to the phase lead characteristics, than the one in the macro region.

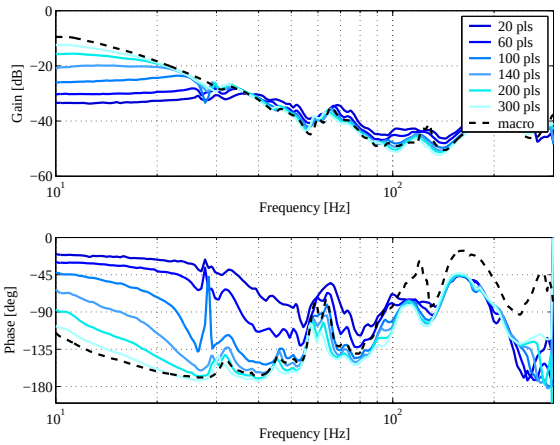

Fig. 10. Bode plots of motor position for motor torque in micro region

Table 4. Parameters of feedback controller

	case-1 (conv.)	case-2	case-3
K_{pp} [rad/s]	73.00	200.0	200.0
K_{sp} [kgm^2/s]	0.151	0.200	0.200
K_{si} [kgm^2/s^2]	10.07	30.00	50.00

Table 5. Gain and phase margins in micro region

	case-1 (conv.)	case-2	case-3
gain margin [dB]	10.89	7.90	7.81
phase margin [deg]	107.76	50.08	38.11

4 FEEDBACK CONTROLLER DESIGN IN MICRO REGION

4.1 Feedback Controller Parameters and Frequency Analyses

From the above examinations on frequency characteristics with the nonlinear friction properties, high gain controllers to expand the control servo bandwidth can be applied to the feedback system, since the phase lead characteristics in low frequency range appear for the micro-displacement motion. Here, alternative two cases of feedback controller parameters (cases-2 and 3) were designed rather than the conventional case (case-1), as listed in Table 4. A specified index for the parameter design is that the gain of sensitive function for the feedback loop becomes lower than 5 dB in all frequency range, from viewpoints of disturbance suppression by the expansion of servo bandwidth.

Figure 11, Table 5, and Figs.12 and 13 show comparative frequency analyses for three cases of feedback parameters in the micro region: Nyquist plots in Fig. 11, gain

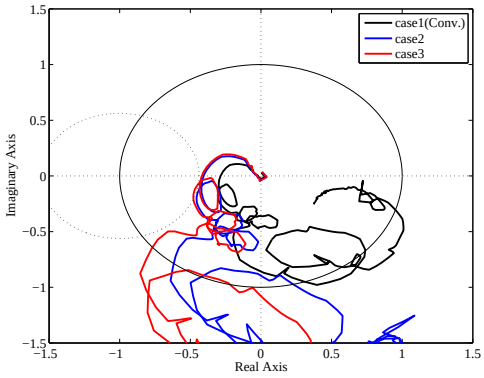

Fig. 11. Nyquist plots in micro region

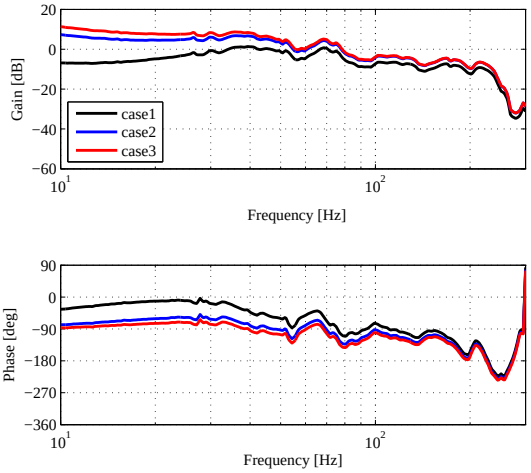

Fig. 12. Open loop characteristics in micro region

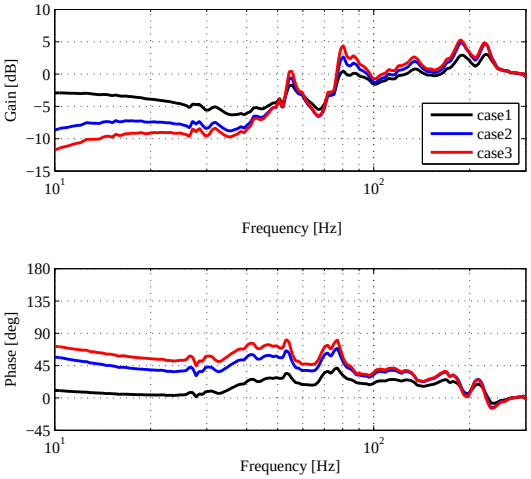

Fig. 13. Sensitivity characteristics of feedback system in micro region

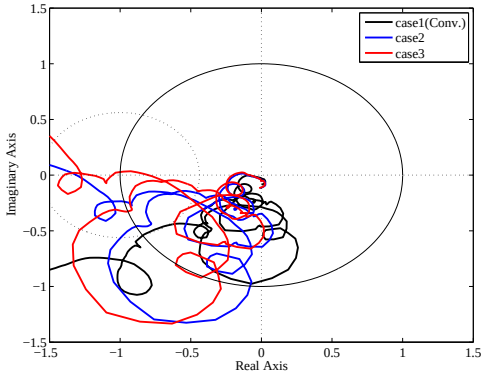

Fig. 14. Nyquist plots in macro region

and phase margins of the feedback system in Table 5, open loop characteristics in Fig. 12, and sensitivity characteristics of the feedback loop in Fig. 13, where all plots and indexes are calculated on the basis of the plant frequency characteristic for 20 pulses in Fig. 10. A dotted circle in the Nyquist plots of Fig. 11 corresponds to the gain of 5 dB in the sensitive function, in order to verify the design specification. According to the above frequency analyses, alternative feedback parameters in cases-2 and 3 can achieve the wider servo bandwidth (from Fig. 12) and the higher disturbance suppression capability in low frequency range (from Figs.11 and 13), under the stable conditions with the desired gain of sensitivity function.

Nyquist plots in Fig. 14 and gain/phase margins in Table 6, on the other hand, show comparative frequency analyses for three cases in the macro region, where those are calculated by the macro-displacement plant characteristic indicated by broken lines in Fig. 10. From the comparison between Figs.11 and 14, the system stability becomes low in the macro region, while the parameters in case-3 especially lead to the unstable system.

Table 6. Gain and phase margins in macro region

	case-1 (conv.)	case-2	case-3
gain margin [dB]	14.81	14.80	1.90
phase margin [deg]	32.71	14.02	-1.83

4.2 Stability Evaluations by Time Responses

In order to verify the system stabilities by time responses of positioning, reciprocation and inching motions are evaluated, where an amplitude of reference r is set as of 40 pulses and a positioning interval time is set as of 4400 sampling periods, respectively. Figure 15 shows response

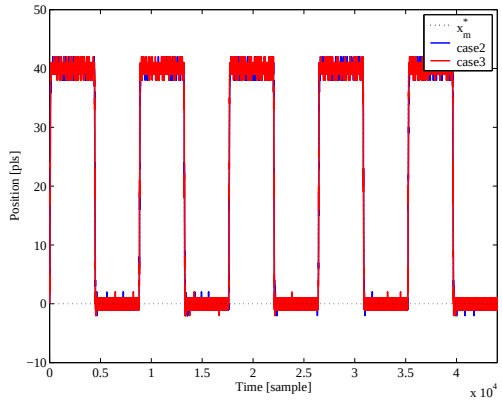

Fig. 15. Response waveforms of motor position for reciprocating motion in micro region (reference amplitude of 40 pulses and interval time of 4400 sample)

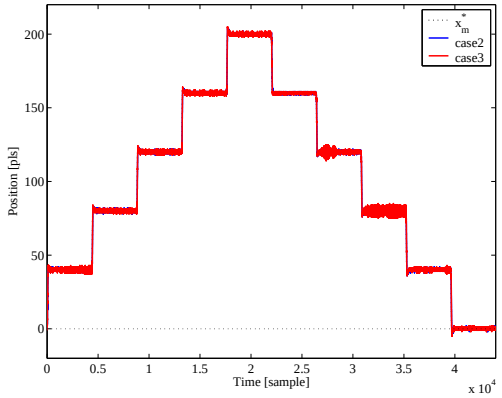

Fig. 17. Response waveforms of motor position for inching motion in micro region (reference amplitude of 40 pulses and interval time of 4400 sample)

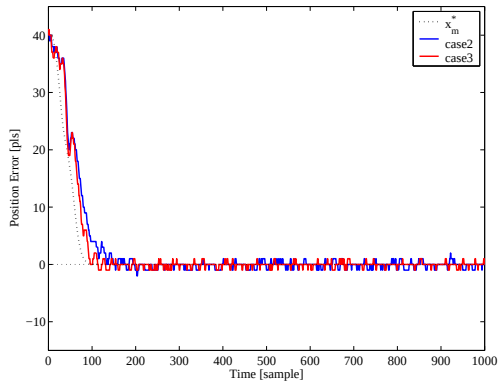

Fig. 16. Magnified response waveforms of motor position error for reciprocating motion in micro region

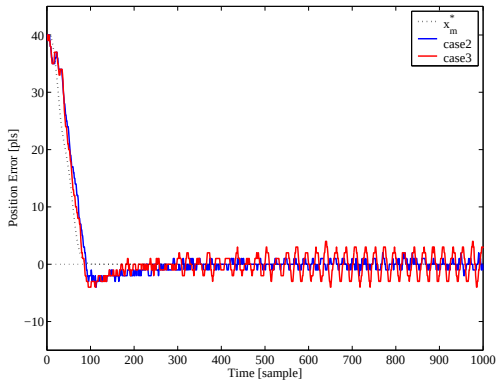

Fig. 18. Magnified response waveforms of motor position error for inching motion in micro region

waveforms for the reciprocating motion, where blue line indicates the response in case-2 and red line indicates the one in case-3. Figure 16 shows magnified response waveforms of the positioning error ($r - x_m$) in one of settling motions of Fig. 15. From the figures, the alternative parameters in cases-2 and 3 give the desired fast and precise positioning performance with stable responses.

Figure 17, on the other hand, shows response waveforms of the inching motion in cases-2 and 3. In the figure, comparing to the responses of Fig. 15 in the case of reciprocating motion, the settling responses of case-3 in the second and third backward motions (at around 2.6 and 3.0×10^4 samples) include vibratory waveforms, while magnified responses in Fig. 18 are extracted from the responses in the third backward motion. These vibratory responses in case-3 suggest that the plant dynamics behave in different ways from ones in Fig. 10, although the system stability is ensured as in Fig. 11. In order to examine the vibratory behaviors, rolling friction responses during the inching motions were measured as shown in Fig. 19. In the figure, the rolling friction level rushes into Coulomb friction as the inching displacement proceeds, that is, the friction as well as the plant dynamics shift to the ones in the macro region, unlike the behaviors during the reciprocating motions in which the displacement does not proceed. As a result, the settling performance might include the vibratory responses depending on the displacement which determines the rolling friction.

According to the above analyses and examinations, the feedback controller parameters should be designed to satisfy the system stability in both micro and macro regions. As a proposed practical design, therefore, the parameters of case-2 are adopted to the feedback controller in the following experimental evaluations.

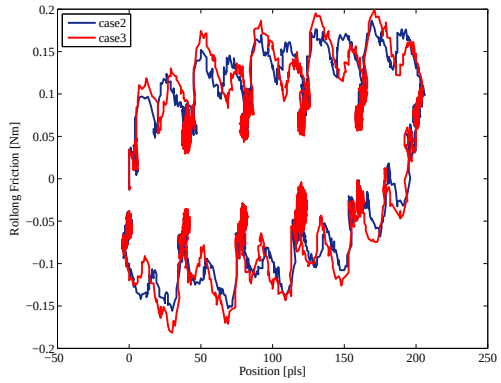

Fig. 19. Rolling friction responses during inching motion (reference amplitude of 40 pulses)

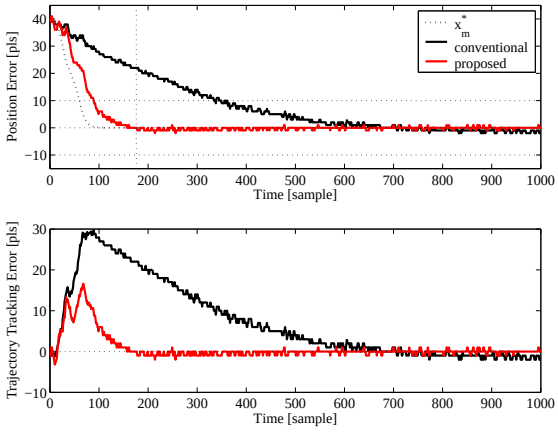

Fig. 20. Comparative response waveforms by feedback parameters of case-2 in micro region (reference amplitude of 40 pulses)

5 EXPERIMENTAL VERIFICATIONS

The same S-shaped motor position responses as in section 2.3 were given to experimentally verify the proposed feedback controller design. Figure 20 shows response waveforms of position error (top) and trajectory tracking error (bottom) in the micro region, while a response waveform of position error in the macro region is given in Fig. 21. Vertical dotted lines in the figures indicate the target settling time. From the figures, the position responses in both micro and macro regions satisfy the required settling performance. In the micro motion case of Fig. 20, the faster settling with 102 samples and the trajectory tracking error within 16 pulses during the motion can be especially achieved in the proposed design, because of the improvement of the sensitivity characteristic by the feedback parameters.

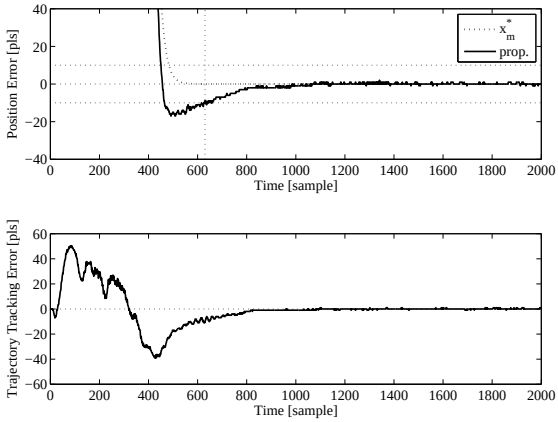

Fig. 21. Magnified response waveform of motor position error by feedback parameters of case-2 in macro region (reference amplitude of 4000 pulses)

6 CONCLUSIONS

This paper proposed the feedback controller design approach considering the plant dynamics of the table system in the micro region. According to the design, the feedback controller parameters should be designed to ensure the system stability in both micro and macro regions from viewpoints of the nonlinear behaviors of rolling friction in the regions. The effectiveness of the proposed design has been experimentally verified using the prototype of ball screw-driven table positioning system, where the required fast and precise positioning performance could be achieved by adopting the proposed design parameters to the feedback controller.

A series of examinations and the controller design for the micro-displacement positioning in this research should be also practically available to the conventional control frameworks to improve the settling performance, e.g., well-known mode switching control.

REFERENCES

[1] S. Futami, A. Furutani, and S. Yoshida: “Nanometer Positioning and Its Micro-Dynamics”, *Nanotechnology*, 1, pp.31-37, 1990.

[2] J. Otsuka and T. Masuda: “The Influence of Nonlinear Spring Behavior of Rolling Elements on Ultraprecision Positioning Control Systems”, *Nanotechnology*, 9, pp.58-92, 1998.

[3] M. Iwasaki, K. Seki, and Y. Maeda: “High Precision Motion Control Techniques -A Promising Approach to Improving Motion Performance”, *IEEE Industrial Electronics Magazine*, Vol.6, No.1, pp.32-40, 2012.

[4] V. Lampaert, J. Swevers, and F. Al-bender: “Experimental Comparison of Different Friction Models for Accurate

Low-Velocity Tracking", *Proc. of the 10th Mediterranean Conference on Control and Automation*, Lisbon, 2002.

[5] J.-S. Chen, K.-C. Chen, Z.-C. Lai, and Y.-K. Huang: "Friction Characterization and Compensation of A Linear-Motor Rolling-Guide Stage", *International Journal of Machine Tools and Manufacture*, Vol.43, pp.905-915, 2003.

[6] Z. Jamaludin, H. Van Brussel, and J. Swevers: "Friction Compensation of an XY Feed Table Using Friction-Model-Based Feedforward and an Inverse-Model-Based Disturbance Observer", *IEEE Trans. on Industrial Electronics*, Vol. 56, No.10, pp.3840-3847, 2009.

[7] H. Asaumi and H. Fujimoto: "Proposal on Nonlinear Friction Compensation Based on Variable Natural Length Spring Model", *SICE Annual Conference*, Tokyo, pp.2393-2398, 2008.

[8] W. Maebashi, K. Ito and M. Iwasaki: "Robust Fast and Precise Positioning with Feedforward Disturbance Compensation", *Proc. of the 37th Annual Conference of the IEEE Industrial Electronics Society*, Melbourne, pp.3299-3304, 2011.

[9] Y. Maeda and M. Iwasaki: "Improvement of Settling Performance by Initial Value Compensation Considering Rolling Friction Characteristics", *Proc. of the 36th Annual Conference of the IEEE Industrial Electronics Society*, Glendale, pp.1902-1907, 2010.

[10] T. Koizumi and O. Kuroda: "Analysis of Damped Vibration of a System with Rolling Friction Rolling Friction Depends on the Displacement", *Journal of Japanese Society of Tribologists*, Vol.35, No.6, pp.435-439 1990. (in Japanese)

[11] T. Umeno and Y. Hori; "Robust speed control of DC servomotors using modern two-degrees-of-freedom controller design,", *IEEE Trans. on Industrial Electronics*, Vol.38, pp.363-368, 1991.

Wataru Maebashi received the B.S. and M.S. degrees in computer science and engineering from Nagoya Institute of Technology, Nagoya, Japan, in 2009 and 2011, respectively. He is now a candidate toward the Dr.Eng. degree at Nagoya Institute of Technology, and is interested in the research on controller design for fast and precise positioning of mechatronic systems.
Mr. Maebashi is a member of the Institute of Electrical Engineering of Japan.

Kazuaki Ito received the B.S., M.S., and Dr.Eng. degrees in electrical and computer engineering from Nagoya Institute of Technology, Nagoya, Japan, in 1998, 2000, and 2003 respectively. In 2003, he joined the Department of Electrical and Electronic Engineering, Toyota National College of Technology, Toyota, Japan, where he is currently an Associate Professor. His current research interests are applications of control techniques to mechatronic systems.
Dr. Itoh is a Member of the Institute of Electrical Engineering of Japan, Japan Society for Precision Engineering, and the Institute of Electrical and Electronics Engineers.

Makoto Iwasaki received the B.S., M.S., and Dr.Eng. degrees in electrical and computer engineering from Nagoya Institute of Technology, Nagoya, Japan, in 1986, 1988, and 1991, respectively. He joined the Department of Electrical and Computer Engineering, Nagoya Institute of Technology in 1991, where he is currently a Professor. His current research interests are applications of control theory and soft computing techniques to motor/motion control, especially to the precise modeling and controller design in the application areas of the fast and precise positioning in industrial mechatronic systems. He contributes as an AdCom Member of IEEE/IES and a Technical Editor for the IEEE/ASME Transactions on Mechatronics.
Prof. Iwasaki is a member of the Institute of Electrical Engineering of Japan, the Japan Society for Precision Engineering, and the Institute of Electrical and Electronics Engineering.

AUTHORS' ADDRESSES

Wataru Maebashi, M.Sc.
Prof. Makoto Iwasaki, Ph.D.
Department of Electrical and Computer Engineering,
Faculty of Engineering,
Nagoya Institute of Technology,
Gokisocho, Showaku, JP-466-8555, Nagoya, Japan
email: maebashi.wataru@nitech.ac.jp, iwasaki@nitech.ac.jp

Assoc. Prof. Kazuaki Ito, Ph.D.
Department of Electrical and Electronic Engineering,
Toyota National College of Technology,
Aichi Prefecture, Toyota, Japan
email: kazu-it@toyota-ct.ac.jp

Received: 2012-06-30
Accepted: 2012-10-15